# Vapor-Phase Infrared Laser Spectroscopy: From Gas Sensing to Forensic Urinalysis

**ARTICLE** *in* ANALYTICAL CHEMISTRY · AUGUST 2008

Impact Factor: 5.64 · DOI: 10.1021/ac8001897 · Source: PubMed

*Anal. Chem.* **2008,** *80,* 5334–5341

# Vapor-Phase Infrared Laser Spectroscopy: From Gas Sensing to Forensic Urinalysis

**Richard Bartlome,* Julien M. Rey, and Markus W. Sigrist***

*Institute for Quantum Electronics, ETH Zurich, Schafmattstrasse 16, 8093 Zurich, Switzerland*

**Numerous gas-sensing devices are based on infrared laser spectroscopy. In this paper, the technique is further developed and, for the first time, applied to forensic urinalysis. For this purpose, a difference frequency generation laser was coupled to an in-house-built, high-temperature multipass cell (HTMC). The continuous tuning range of the laser was extended to 329 $cm^{-1}$ in the fingerprint C−H stretching region between 3 and 4 $\mu$m. The HTMC is a long-path absorption cell designed to withstand organic samples in the vapor phase (Bartlome, R.; Baer, M.; Sigrist, M. W. *Rev. Sci. Instrum.* 2007, *78*, 013110). Quantitative measurements were taken on pure ephedrine and pseudoephedrine vapors. Despite featuring similarities, the vapor-phase infrared spectra of these diastereoisomers are clearly distinguishable with respect to a vibrational band centered at 2970.5 and 2980.1 $cm^{-1}$, respectively. Ephedrine-positive and pseudoephedrine-positive urine samples were prepared by means of liquid−liquid extraction and directly evaporated in the HTMC without any preliminary chromatographic separation. When 10 or 20 mL of ephedrine-positive human urine is prepared, the detection limit of ephedrine, prohibited in sports as of 10 $\mu$g/mL, is 50 or 25 $\mu$g/mL, respectively. The laser spectrometer has room for much improvement; its potential is discussed with respect to doping agents detection.**

Illegal doping substances taken by athletes are currently detected in urine using primarily gas chromatography coupled to mass spectrometry (GC/MS) and liquid chromatography coupled to mass spectrometry (LC/MS).[1–7] Complementary methods are required to confirm positive findings with better accuracy and to provide courts with more reliable scientific evidence. Several challenges are faced today in doping agents analysis such as (i) differentiation between substances of endogenous and exogenous origin, (ii) structural differentiation, and (iii) the reduction of the time needed to perform a test.

The purpose of this study is to investigate the potential of a novel complementary method—based on infrared (IR) laser spectroscopy—that does not require chromatographic separation to differentiate between closely related chemical structures such as isomers. The IR spectrum is a unique identification characteristic of molecules that does not only depend on the particular functional groups but that also reflects the arrangement of these functional groups within the molecule. Unlike spectra obtained by mass spectrometry, the IR spectrum is predominantly a property of the whole molecule rather than the sum of the properties of its constituents.

Infrared spectra can be recorded in the vapor, liquid, or solid phase. In contrast to the vapor phase, quantitative measurements are difficult in the solid phase due to scattering effects, whereas liquid-phase spectra tend to be broad and unselective. In this research, vapor-phase spectra were recorded with an in-house-built laser spectrometer.

According to a gas chromatography-Fourier transform infrared study, the wavelength range between 2.7 and 3.9 $\mu$m (2550−3750 $cm^{-1}$) has been identified as a fingerprint region for various drugs of abuse, along with the wavelength range between 5 and 17 $\mu$m (600−2000 $cm^{-1}$).[8]

Infrared laser spectroscopy—aimed at fingerprinting rather large organic molecules such as doping agents in urine—requires wide continuous tuning of the laser wavelength. Promising broadly tunable mid-IR laser sources—that do not require cryogenic cooling— include $Cr^{2+}$-doped solid-state lasers in the mid-IR below 3 $\mu$m,[9,10] external-cavity quantum-cascade lasers in the mid-IR range above 4 $\mu$m,[11,12] optical parametric oscillators,[13–15] and difference frequency generation (DFG) sources.[15,16] A DFG laser was further developed in this research to reach the 3−4-$\mu$m fingerprint region, where fundamental C−H stretching vibrations can be excited.

Samples were evaporated in an in-house-built, high-temperature multipass cell (HTMC) pictured in Figure 1. The HTMC is a novel heatable long-path absorption cell, where the mirrors are sepa-

* To whom correspondence should be addressed. E-mail: richard.bartlome@alumni.ethz.ch (R.B.); sigrist@iqe.phys.ethz.ch (M.W.S.).

(1) Bartlome, R.; Baer, M.; Sigrist, M. W. *Rev. Sci. Instrum.* **2007**, *78*, 013110.
(2) Hemmersbach, P.; de la Torre, R. *J. Chromatogr., B* **1996**, *687*, 221.
(3) Maurer, H. H. *J. Mass Spectrom.* **2006**, *41*, 1399.
(4) Maurer, H. H. *J. Chromatogr., B* **1998**, *713*, 3.
(5) Politi, L.; Groppi, A.; Polettini, A. *J. Anal. Toxicol.* **2005**, *29*, 1.
(6) Thevis, M.; Schanzer, W. *Curr. Org. Chem.* **2005**, *9*, 825.
(7) Thevis, M.; Schanzer, W. *Mass Spectrom. Rev.* **2007**, *26*, 79.
(8) Praisler, M.; Van Bocxlaer, J.; De Leenheer, A.; Massart, D. L. *J. Chromatogr., A* **2002**, *962*, 161.
(9) Sorokina, I. T.; Sorokin, E.; Di Lieto, A.; Tonelli, M.; Page, R. H.; Schaffers, K. I. *J. Opt. Soc. Am. B* **2001**, *18*, 926.
(10) Sorokina, I. T. In *Solid-state mid-infrared laser sources*; Sorokina, I. T., Vodopyanov, K. L., Eds.; Springer: New York, 2003; Vol. 89, pp 255−350.
(11) Wysocki, G.; Curl, R. F.; Tittel, F. K.; Maulini, R.; Bulliard, J. M.; Faist, J. *Appl. Phys. B: Lasers Opt.* **2005**, *81*, 769.
(12) Maulini, R.; Yarekha, D. A.; Bulliard, J. M.; Giovannini, M.; Faist, J. *Opt. Lett.* **2005**, *30*, 2584.
(13) Ebrahimzadeh, M. In *Solid-state mid-infrared laser sources*; Sorokina, I. T., Vodopyanov, K. L., Eds.;Springer,:New York, 2003; Vol. 89, pp 179−218.
(14) Ngai, A. K. Y.; Persijn, S. T.; von Basum, G.; Harren, F. J. M. *Appl. Phys. B: Lasers Opt.* **2006**, *85*, 173.
(15) Waechter, H.;Sigrist, M. W. In *Springer Handbook of Lasers and Optics*; Träger, F., Ed.; Springer: New York, 2007; Chapter 11.10.



10.1021/ac8001897 CCC: $40.75 
Published on Web 06/18/2008

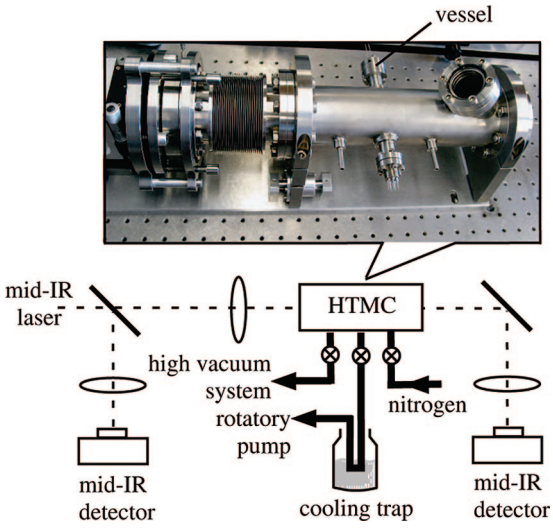


**Figure 1.** Tunable mid-IR laser beam, generated by means of DFG, coupled into the HTMC pictured above. Experimental details of the DFG system and the HTMC were previously published.[1]

rately heated in order to avoid condensation on their optical surface.[1] To prevent fatal optical misalignments, the cell is also designed to compensate thermal expansion by the simultaneous action of a bellows and linear bushings. Since no cold spots appear on the inner surface of the HTMC, measurements on condensable vapors are feasible, in addition to traditional gas measurements. All materials in contact with the samples have good resistance to aggressive chemicals.

The HTMC, combined with the widely and continuously tunable DFG radiation, offers a unique analytical tool for probing liquid and solid organic samples in the vapor phase. The reliability of the laser spectrometer and its wide tunability were demonstrated by recording the whole C−H stretching absorption band of acetone vapor at 296, 400, and 500 K.[17] Unlike conventional FT-IR spectroscopy, the presence of narrow water vapor absorption lines has a negligible influence on the measured contour of an absorption band thanks to the narrow line width of the laser source.

The majority of quantitative vibrational analyses have targeted the main urine constituents. Urea, creatinine, uric acid, sulfate, phosphate, glucose, and protein content have been quantified by Raman and FT-IR studies.[18–23] The presence of doping agents among all these components usually requires sample preparation and chromatographic separation. Recently, a near-infrared Raman spectrometer has detected ephedrine at relevant concentrations directly in urine.[24] It was not reported whether the spectrometer resolution would be sufficient to differentiate between closely related structures such as ephedrine and pseudoephedrine. In this work, prepared ephedrine- and pseudoephedrine-positive urine samples were directly investigated with the novel laser spectrometer mentioned above. Quantitative measurements were also taken on pure ephedrine, pure pseudoephedrine, and main urine constituents.

**Ephedrine and Pseudoephedrine.** Ephedrine and pseudoephedrine are stereoisomers (spatial isomers) of 2-methylamino-1-phenylpropanol ($C_{10}H_{15}NO$); i.e., they share the same bonds and have identical atoms sharing the same neighbors. The structural formula of 2-methylamino-1-phenylpropanol has two carbon chiral centers. Each may assume an *R* and *S* configuration, so there are four stereoisomeric combinations possible. These are shown in Figure 2, together with the assignments made on the basis of chemical interconversions.

Ephedrine and pseudoephedrine reveal significantly different physical properties: ephedrine has a melting point of 36 °C, is moderately soluble in water, and has a specific optical rotation $[\alpha]_D^{22}$ of ± 3° in EtOH, whereas pseudoephedrine has a melting point of 116 °C, is sparingly soluble in water, and has a specific optical rotation $[\alpha]_D^{22}$ of ± 53° in EtOH.[25] While ephedrine has been banned from sports for its stimulatory effects, pseudoephedrine has different pharmacological properties and is considered as legal. The World Anti-Doping Code prohibits ephedrine when its concentration in urine is >10 $\mu$g/mL.[26] A sensitive and selective analytical method is therefore required to differentiate between these two isomers in urine.

## EXPERIMENTAL SECTION

**Laser Spectrometer.** A DFG laser, previously described,[1] was further developed essentially with respect to its continuous tuning range. The basic optical arrangement remains unchanged: a *Q*-switched Nd:YAG laser (Innolight GmbH, Hannover, Germany) serves as a pump beam, while the signal beam is provided by a continuous-wave external-cavity diode laser (ECDL) (Santec, Komaki, Aichi, Japan). The Nd:YAG laser delivers 6-ns short pulses at a peak power of 5 kW and at a frequency repetition rate of 4−8 kHz. The ECDL is fiber-coupled and equipped with an optical isolator to prevent disturbances from possible back-reflections. About 1% of the ECDL beam power is coupled into a wavemeter (Burleigh Instruments, Fishers, NY) for constant control of the signal wavelength $\lambda_s$. The pump wavelength $\lambda_p$ was determined in a previous work as a function of the Nd:YAG crystal temperature.[27] The wavelength $\lambda_i$ of the mid-IR idler beam is permanently controlled with an accuracy of 0.01 $cm^{-1}$, as it must satisfy the energy conservation law $1/\lambda_i = 1/\lambda_p - 1/\lambda_s$. Difference frequency conversion—from the pump and signal beam into the mid-IR idler beam—takes place in one of two grating periods of a temperature-controlled 50-mm-long periodically poled lithium niobate crystal (PPLN). A small portion of the pump beam is

(16) Fischer, C.; Sigrist, M. W. In *Solid-state mid-infrared laser sources*; Sorokina, I. T.; Vodopyanov, K. L., Eds.; Springer: Berlin, 2003; Vol. 89, pp 97−140.
(17) Sigrist, M. W.; Bartlome, R.; Marinov, D.; Rey, J. M.; Vogler, D. E.; Wächter, H. *Appl. Phys. B: Lasers Opt.* **2008**, *90*, 289.
(18) Hoşafçi, G.; Klein, O.; Oremek, G.; Mäntele, W. *Anal. Bioanal. Chem.* **2007**, *387*, 1815.
(19) Petrich, W. *Appl. Spectrosc. Rev.* **2001**, *36*, 181.
(20) Premasiri, W.; Clarke, R.; Womble, M. *Lasers Surg. Med.* **2001**, *28*, 330.
(21) Heise, H. M.; Voigt, G.; Lampen, P.; Küpper, L.; Rudloff, S.; Werner, G. *Appl. Spectrosc.* **2001**, *55*, 434.
(22) Shaw, R. A.; Low-Ying, S.; Leroux, M.; Mantsch, H. H. *Clin. Chem.* **2000**, *46*, 1493.
(23) Doua, X.; Yamaguchia, Y.; Yamamotoa, H.; Doia, S.; Ozakib, Y. *Vib. Spectrosc.* **1996**, *13*, 83.
(24) Guimaraes, A.; Pacheco, M., Jr.; Barsottini, D.; Duarte, J.; Villaverde, A.; Zangaro, R. *Spectroscopy* **2006**, *20*, 185.
(25) Lyle, G. G. *J. Org. Chem.* **1960**, *25*, 1779.
(26) The World Anti-Doping Code—The 2007 Prohibited List—International standard; World Anti-Doping Agency, 2006; http://www.wada-ama.org.
(27) Fischer, C.; Wettstein, E.; Sigrist, M. W. *Appl. Phys. B: Lasers Opt.* **2001**, *73*, 233.

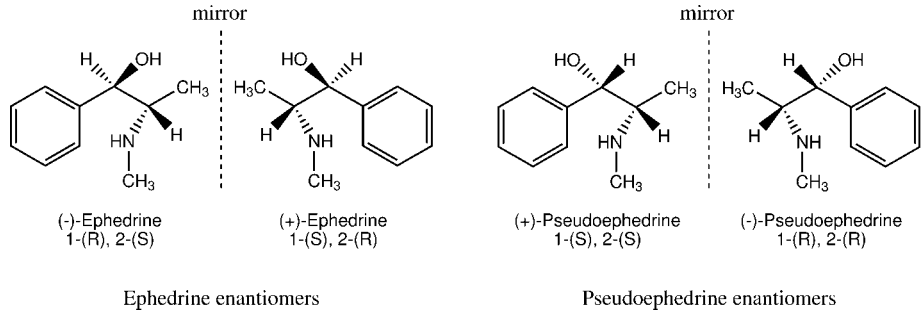


**Figure 2.** Stereoisomers of 2-methylamino-1-phenylpropanol. (−)-ephedrine and (+)-pseudoephedrine are found in the Chinese shrub Ma Huang (*Ephedra vulgaris*). (+)-Ephedrine and (−)-pseudoephedrine can be synthesized.

collected for the purpose of a trigger signal. After the PPLN, a germanium filter lets only the mid-IR idler beam pass through. A pinhole is placed after the PPLN to spatially clean the DFG beam. Preliminary measurements have shown that such a pinhole makes the setup considerably less sensitive to crystal temperature fluctuations, which currently limit the instrumental noise to 0.3−0.5% (transmission scale).

The DFG source has a narrow line width of only 150 MHz ($5 \times 10^{-3}$ cm$^{-1}$).[28] In gas-sensing applications, such devices are finely tuned within a narrow range of 1−2 cm$^{-1}$.[29] To meet our requirements, the continuous tuning range of the DFG radiation was extended to 329 cm$^{-1}$ with a step width of 0.04−0.4 cm$^{-1}$. Such a broad tuning range was achieved by simultaneously tuning the step motor of the ECDL and the temperature of the PPLN. The tuning mechanism is fully automated. The optimal temperature of the PPLN was determined during preliminary measurements. The accessible idler wavelength range (2815−3144 cm$^{-1}$) is only limited by the tuning range of the ECDL (1520−1600 nm).

The idler beam is split by a $CaF_2$ window before entering the HTMC[1] pictured in Figure 1. The mid-IR power entering and exiting the HTMC is recorded by two thermoelectrically cooled Hg−Cd−Zn−Te detectors (Vigo System S.A., Warsaw, Poland). The transmitted and reflected portions of the beam after the splitter travel approximately the same distance in open space before reaching the detectors. This arrangement prevents unwanted absorption lines in the background due to the presence of absorbing species in ambient air.

To avoid fringes, optical elements such as the beam splitter or the entry window of the HTMC are wedged. However, a distinctive fringe pattern with a period $\Delta\tilde{\nu} = 3.8$ cm$^{-1}$ may still subsist. It is due to a 800-$\mu$m-thick $BaF_2$ protective window mounted in front of each detector. These fringes can be reduced by adjusting the detectors in a way that multiple reflections within the $BaF_2$ window no longer overlap and do not interfere with each other. When the transmission is calculated in routine measurements, fringes can be canceled out in most cases.

As the DFG efficiency may vary across the wide tuning range, an automated scale change is implemented for optimal data acquisition of the detector signals with an oscilloscope (TDS 644A, Tektronix). One hundred and fifty pulses per step are averaged on the oscilloscope.

The cell has a total inner volume of 2.0 L, including all fittings, valves, and a high-temperature-resistant pressure transducer. The total optical path length can be varied from about 9 to 35 m depending on the number of laser beam passes inside the HTMC.[1]

An in-house-built rack, consisting of four proportional integral derivative temperature controllers, monitors the mirror heaters of the HTMC, the wire heater of the cell body, and the ring heater of the vessel separately. In this way, the temperature of the cell, the mirrors, and the vessel can be adjusted between room temperature and 573 K with an accuracy of 1 K. The maximum achievable temperature of 573 K is limited here by the total heating power available and not by the materials used.

After each measurement cycle, condensates are captured in a cooling trap prior to evacuating the cell through a high-vacuum system. Background measurements with pure nitrogen (99.999%) are performed before or after each measurement series. To prevent oxidation of the mirrors at elevated temperatures, nitrogen rather than synthetic air is always employed as nonabsorbing buffer gas.

**Sample Preparation.** Pure samples such as ephedrine, pseudoephedrine and urea were directly introduced into the vessel and evaporated in the HTMC. Urine samples required sample preparation. Sample preparation is an essential step, because most analytical instruments cannot handle a sample matrix directly. Current sample preparation procedures rely on standard liquid−liquid extraction, solid-phase extraction,[30] solid-phase microextraction,[31,32] and stir bar sorptive extraction.[33] In the following, we adapted a liquid−liquid extraction procedure to prepare urine samples. Preliminary studies served to select the most suitable solvent and the optimal number of solvent batches for extraction. Urine samples were prepared according to the following steps:

**(1) Collection of 10 mL of Human Urine**. Fresh negative (i.e., blank) human urine samples came from well-known personnel claiming abstinence from drugs; positive human urine samples were obtained by adding the desired amount of analyte to the urine sample. All samples were prepared shortly after collection. Larger urine volumes result in larger extracted amounts. In general, urine is screened for different compounds. When a urine specimen is sent to a forensic laboratory, it is divided into several batches; each batch undergoes a specific preparation. The volume of a single batch must therefore not exceed 10 or 20 mL.

(28) Seiter, M.; Sigrist, M. W. *Opt. Lett.* **1999**, *24*, 110.
(29) Richter, D.; Fried, A.; Wert, B. P.; Walega, J. G.; Tittel, F. K. *Appl. Phys. B: Lasers Opt.* **2002**, *75*, 281.
(30) Supelco. Guide to solid phase extraction; Sigma-Aldrich, 1998.
(31) Arthur, C. L.; Pawliszyn, J. *Anal. Chem.* **1990**, *62*, 2145.
(32) Vas, G.; Vékey, K. *J. Mass Spectrom.* **2004**, *39*, 233.
(33) Baltussen, E.; Sandra, P.; David, F.; Cramers, C. *J. Microcolumn Sep.* **1999**, *11*, 737.

**(2) Adjustment to Alkaline pH.** The pH of urine, normally situated between 4.5 and 8, was increased to more than 12 by adding NaOH 10 M.

**(3) Multiple Extraction with 8 Batches of 2.5 mL of chloroform (20 mL in total).** Another frequently used extraction solvent is *tert*-butyl methyl ether (bp 55 °C).[34,35] Chloroform was chosen instead, because it has a lower solubility in water (8 g/L instead of 50 g/L) and is as easy to evaporate (bp 61 °C). Furthermore, chloroform does not present any significant absorption feature in the C−H stretching region, unlike ethers. This has also been confirmed by a preliminary measurement on pure chloroform.

**(4) Centrifugation at 2000g during 2 min.** Before centrifugation, the water−chloroform interface is not clearly defined. The presence of albumin in urine is responsible for an intermediary chloroform−water emulsion. This emulsion was broken by centrifugation.

**(5) Solvent Evaporation and Transfer to the HTMC Vessel.** The eight batches of extraction solvent were put together in one flask. The chloroform was then slowly evaporated. The last few drops were transferred to a sample holder designed to fit inside a small vessel mounted on a Conflat flange. The chloroform was left to evaporate in ambient air. The flange, around which a ring heater can be tightened, was sealed to the HTMC. Two electric feed-throughs are welded to the flange to control the temperature of the vessel. All samples were placed in this vessel prior to evaporation in the cell.

**Absorption Cross Section.** The absorbance $A$ is determined by the total density of species $n$ present in the cell, the effective absorption cross section per molecule in the cell $\tilde{\sigma}$, and the absorption path length $L$:

$$A = n\tilde{\sigma}L \qquad (1)$$

It follows from this definition that the absorbance is given in terms of the *natural* logarithm in the Beer−Lambert's law. This is the physical quantity we refer to in cross-section measurements presented throughout this work. Frequency integration of $\tilde{\sigma}$ yields the temperature-dependent line intensity as defined in units of reciprocal centimeters/(molecule × cm$^{-2}$) in the Hitran database.[36] (The effective absorption cross section $\tilde{\sigma}$ must not be confused with the usual definition of the absorption cross section $\sigma$, the frequency integration of which yields a temperature-independent quantity related to the Einstein coefficient.)

## RESULTS AND DISCUSSION

**IR Spectroscopy of Ephedrine and Pseudoephedrine.** Pure (+)-ephedrine was not investigated because it was only available in its hydrochloride or hemihydrate form. In Figure 3, vapor-phase IR measurements of (−)-ephedrine, (+)-pseudoephedrine, and (−)-pseudoephedrine (Sigma-Aldrich, Inc.) are compared to each other. They were recorded at 423 K, i.e., above the melting point of pseudoephedrine. For each substance, a small amount was introduced in the vessel to ensure complete evaporation in the HTMC; the partial pressure of a compound at 423 K always stayed below its saturation vapor pressure. In this manner, the measured absorbance at a given wavelength increases linearly as a function of the probe mass introduced in the vessel, as seen in Figure 4.

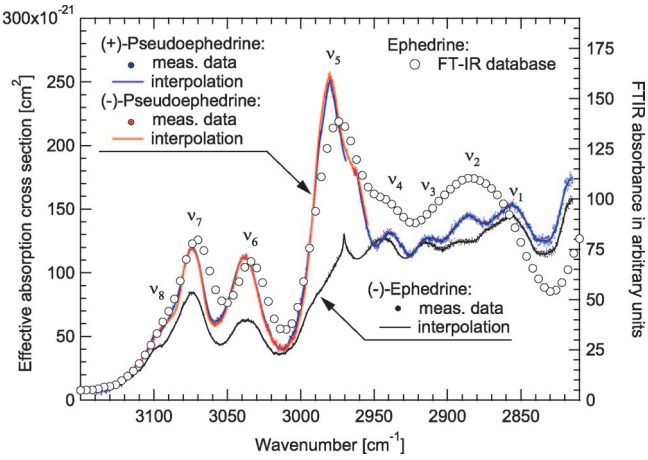


**Figure 3.** C−H stretching absorption band of ephedrine and pseudoephedrine vapor. Quantitative laser-based measurements were taken in 100 mbar $N_2$ at 423 K. The path length of the HTMC was 31.7 m. The DFG laser (line width = 5 × 10$^{-3}$ cm$^{-1}$) was tuned with steps of 0.08 cm$^{-1}$.

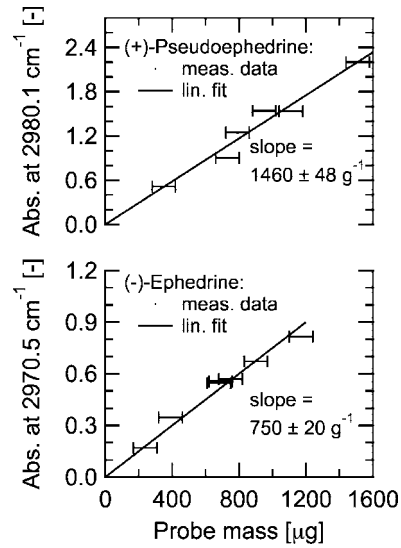


**Figure 4.** Ephedrine and pseudoephedrine detection limits. They are 12 and 6 $\mu$g, respectively (SNR = 3).

The horizontal error bars in Figure 4 depict the reproducibility of the weighing procedure, which is of the order of 70 $\mu$g. From the linear fit, effective cross sections of ephedrine and pseudoephedrine were calculated, as displayed on the *y*-axis of Figure 3. Given an optical path length of 31.7 m and an average noise level of 0.3% (transmission scale), the detection limits of ephedrine and pseudoephedrine are 12 and 6 $\mu$g, respectively (SNR=3).

The vapor-phase IR spectra were recorded over the whole available wavenumber range of 329 cm$^{-1}$ and are compared in Figure 3 to an FT-IR spectrum of ephedrine. The latter was measured in the gas phase at an unspecified temperature and at

(34) Soriano, C.; Munoz-Guerra, J.; Carreras, D.; Rodriguez, C.; Rodriguez, A. F.; Cortés, R. *J. Chromatogr., B* **1996**, *687*, 183.
(35) Van Eenoo, P.; Delbeke, F. T.; Roels, K.; De Backer, P. *J. Chromatogr., B* **2001**, *760*, 255.
(36) Rothman, L. S.; Rinsland, C. P.; Goldman, A.; Massie, S. T.; Edwards, D. P.; Flaud, J.-M.; Perrin, A.; Camy-Peyret, C.; Dana, V.; Mandin, J.-Y.; Schroeder, J.; McCann, A.; Gamache, R. R.; Wattson, R. B.; Yoshino, K.; Chance, K. V.; Jucks, K. W.; Brown, L. R.; Nemtchinov, V.; Varanasi, P. *J. Quant. Spectrosc. Radiat. Transfer* **1998**, *60*, 665.

**Table 1. C−H Stretching Vibrations Bands $\nu_1$−$\nu_8$ of Ephedrine and Pseudoephedrine As Determined from Figure 3**

| | ephedrine | | pseudoephedrine |
|---|---|---|---|
| | FT-IR | DFG | DFG |
| | | 423 K | 423 K |
| | ±8 $cm^{-1}$ | ±0.1 $cm^{-1}$ | ±0.1 $cm^{-1}$ |
| $\nu_1$ | | 2855.8 | 2856.0 |
| $\nu_2$ | 2886 | | 2885.6 |
| $\nu_3$ | | 2915.4[a] | 2913.5[c] |
| $\nu_4$ | | 2942.8 | 2939.4 |
| $\nu_5$ | 2974 | 2970.5 | 2980.1 |
| $\nu_6$ | 3034 | 3037.3[b] | 3038.3 |
| $\nu_7$ | 3070 | 3074.0 | 3074.2[d] |
| $\nu_8$ | | | |

[a] ±0.5 $cm^{-1}$. [b] ±0.9 $cm^{-1}$. [c] ±0.7 $cm^{-1}$. [d] ±0.2 $cm^{-1}$.

a resolution of 8 $cm^{-1}$ by a GC/FT-IR instrument.[37] Such FT-IR data provide only relative absorption coefficients as a function of wavelength unlike quantitative laser-based measurements presented here.

The measured data points were interpolated with a smoothing spline algorithm.[38] All observed bands $\nu_1$ to $\nu_8$ are summarized in Table 1. The interpolation has a profile that allows most of the bands to be determined with an accuracy of 0.1 $cm^{-1}$. Exceptions are indicated separately at the bottom of Table 1. Some bands, such as $\nu_8$, are not strong enough to determine a center frequency with sufficient accuracy.

Except for $\nu_2$, the bands observed by FT-IR match well with those observed with the DFG source. The bands $\nu_1$, $\nu_3$, $\nu_4$, and $\nu_8$ are unresolved as a result of the low FT-IR resolution. Furthermore, other bands appear flattened compared to the laser-based spectrum measured at 423 K. In fact, the FT-IR spectrum should rather be thought of as a convolution between the instrumental resolution and the intrinsic absorption features of ephedrine. Strictly speaking, the FT-IR spectrum is not suitable for comparison purposes as the temperature at which is was recorded is unknown.

The different pressure conditions cannot account for the differences between the FT-IR and the laser-based measurements. Rotovibrational absorption lines of larger molecules such as ephedrine or acetone overlap to form vibrational absorption bands. The contours of such absorption spectra remain unchanged between 0.1 and 1 bar.[17]

As expected, the IR spectra of the pseudoephedrine enantiomers overlap. This also gives an idea of the reproducibility of measurements. The IR spectrum of ephedrine clearly differs from the spectrum of its stereoisomer pseudoephedrine, especially with respect to the band $\nu_5$. The latter is shifted by 9.6 $cm^{-1}$ and is considerably weaker in ephedrine. Together with the derived detection limits in the low-microgram range, the strong discriminating power of the laser spectrometer has motivated further studies with urine samples. The recorded vapor-phase IR spectra are also free from solvent effects, scattering effects, and intermolecular interactions. They feature intrinsic absorption features and are, therefore, particularly suitable for further comparison with ab initio calculations.[39,40]

Water lines may alter spectral profiles. Such impurity effects are problematic in FT-IR recordings. One cannot be certain if some absorption features are due to water or to the species under investigation. Thanks to the narrow line width of the laser source, water absorption lines appeared in this work in the form of isolated data points that significantly deviated from the continuous absorption profile. Around 30 of such data points (out of 4000 recorded) could be unequivocally assigned to water vapor and were deleted from Figure 3.

**Table 2. Urine Composition of Healthy Subjects**

| | normal ranges |
|---|---|
| water | 0.6−2 L/24 h |
| urea | 8−30 g/L |
| inorganic salts | 6−22 g/L |
| creatinine | 0.3−3 g/L |
| uric acid | 0.2−1 g/L |
| glucose | <300 mg/L |
| proteins | <150 mg/L |
| ketone bodies | <50 mg/L |

**Urinalysis.** Urine is a complex aqueous solution whose pH normally varies from 4.5 to 8. Solutes account for ~4% of the total mass. The volume and composition of urine can vary greatly depending on an individual's diet, physical activity, or health, to name a few. Because of these variables, a normal value in urine for each constituent is difficult to establish. In Table 2, normal ranges were defined by comparing different literature sources.[18,21,41–43] Correlations between the individual constituents are not mentioned.

The high water content of biological fluids strongly limits direct mid-IR spectroscopic measurements. For example, in the spectral region accessible by the DFG laser, measurements would be completely hindered if only 10 $\mu$L of water was evaporated in the HTMC. Assuming a cell volume of 2.0 L, this would correspond to 10% water vapor buffered in an ideal gas at 423 K and 100 mbar total pressure. There is hardly any spectral window free from strong water vapor absorption lines. Consequently, initial urine measurements were recorded on dried samples.

Dried human urine was obtained by means of lyophilization (Medichem, Steinenbronn, Germany). A few milligrams of lyophilized urine was placed in the HTMC vessel. The vessel was sealed to the cell, and the latter was evacuated and filled again with 70 mbar nitrogen at room temperature. Measurements were recorded after heating the vessel and the cell to 333 (not pictured), 398 (not pictured), and 423 K (Figure 5), respectively. The mirrors were kept at a slightly higher temperature than the rest of the cell to prevent condensation on their optical surface. The path length was 31.7 m. The DFG source was tuned over 244 $cm^{-1}$ with steps of 0.4 $cm^{-1}$ using only one grating period of the PPLN.


(37) Stein, S. E. In *NIST Chemistry WebBook, NIST Standard Reference Database Number 69*; Linstrom, P. J., Mallard, W. G., Eds.; National Institute of Standards and Technology: Gaithersburg, MD, 2005; http://webbook.nist.gov.

(38) Reinsch, C. H. *Numer. Math.* **1967**, *10*, 177.

(39) Freedman, T.; Ragunathan, N.; Alexander, S. *Faraday Discuss.* **1994**, *99*, 131.

(40) Butz, P.; Kroemer, R. T.; Macleod, N. A.; Simons, J. P. *J. Phys. Chem. A* **2001**, *105*, 544.

(41) Brunzel, N. A. *Fundamentals of urine & body fluid analysis*, 2nd ed.; Saunders: Philadelphia, PA, 2004.

(42) *Professional guide to diagnostic tests*; Lippincott Williams & Wilkins: Ambler, PA, 2004.

(43) McBride, L. J. *Textbook of urinalysis and body fluids: a clinical approach*; Lippincott: Philadelphia, PA, 1998.

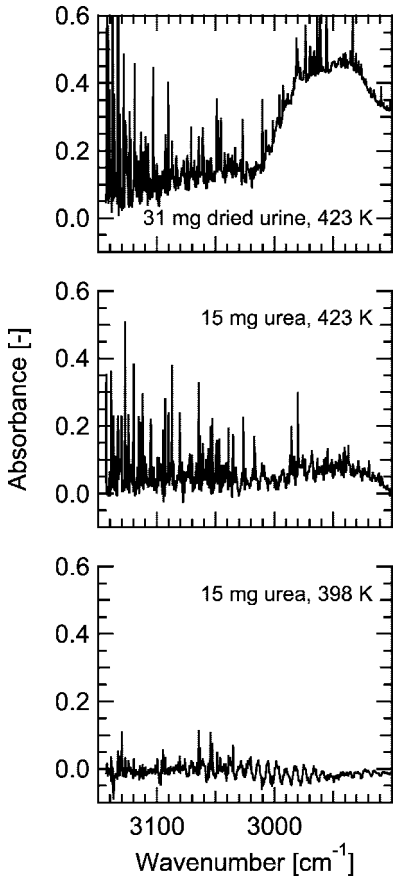


**Figure 5.** Vapor-phase infrared measurements of dried urine and urea. Single scans were taken in 100 mbar $N_2$ at 423 K and in 94 mbar $N_2$ at 398 K. The path length of the HTMC was 31.7 m. The DFG laser was tuned with steps of 0.4 $cm^{-1}$.

As pictured in Figure 5, the vapor-phase spectrum of dried urine taken at 423 K exhibits narrow absorption lines, especially above 3050 $cm^{-1}$. With the help of Hitran,[44] they could be assigned to more than 7000 ppm $H_2O$ and ~3% $NH_3$. Thanks to the narrow line width of the laser ($5 \times 10^{-3}$ $cm^{-1}$), the relatively wide chosen tuning step width of 0.4 $cm^{-1}$ does not hinder the appearance of narrow absorption features—unlike in a conventional FT-IR acquisition. The narrow features in Figure 5 are, however, not spectrally resolved but are merely due to single data points. Such data points may be centered on absorption lines, but may also be situated at the wings of such absorption lines. Therefore, one can only derive a lower limit for the concentration of an absorbing species in the cell. By comparing several data points, one can, however, get a fairly good idea of the concentration of an absorbing species without performing a piezoscan. Furthermore, it is important to understand that the accuracy with which the individual data points are measured (0.01 $cm^{-1}$) is far better than the chosen step width (0.4 $cm^{-1}$), as explained under the section Laser Spectrometer. This level of accuracy does not emerge in Figure 5 but only in the raw data.

Besides narrow lines, a broad absorption appears between 2900 and 3010 $cm^{-1}$. This band is not present at 333 K, but appears at 398 and 423 K. It may be due to the absorption of an organic molecule that has a melting point between 333 and 398 K.

The measurement on dried urine taken at 333 K (not pictured) does not reveal any particular absorption features, apart from three isolated lines due to less than 1000 ppm water vapor. The cell is shortly evacuated before introducing pure $N_2$, and up to 1000 ppm water vapor may subsist in routine measurements. Therefore, the water vapor, at least at 333 K, does not necessarily come from the urine sample itself. However, the increased water vapor concentration at 398 and 423 K may originate from the evaporation of residual water left after the lyophilization process. Ammonia, a gas at room temperature, is not observed at 333 K. It must be due to the breakdown or thermal degradation of a urine constituent. From these initial measurements, we can conclude that ammonia is the limiting factor when recording vapor-phase mid-IR measurements on dried urine samples. To understand the origin of this ammonia, further studies were undertaken on urea, the main solute of urine.

Pure urea (≥99.5%) was purchased from Sigma-Aldrich. It accounts for ~50% of the total mass of solutes in urine (Table 2). Hence, 15 mg was introduced in the vessel, in order to reproduce the amount expected in the 31 mg of dried urine measured previously. The measurement procedure, the wavelength coverage, and the step width were all the same as employed for measurements with dried urine. The urea vapor-phase spectra taken at 398 and 423 K are pictured in Figure 5.

Urea does not have any C−H bond; its IR spectrum does not feature any intrinsic absorption band in the spectral region covered by Figure 5.[45] Besides a fringe artifact between 2960 and 3040 $cm^{-1}$, the measurement at 398 K only exhibits some weak absorption lines. For example, the measured line at 3064.42 $cm^{-1}$ (given by the raw data) was assigned to a water vapor line situated at 3064.404 $cm^{-1}$. It is due to a residual concentration of ≥400 ppm in the cell. In the measurement taken at 423 K, further lines, e.g., measured at 3054.33 or 3080.35 $cm^{-1}$, could not be assigned. Ammonia absorption lines appear as well, in addition to the regular water vapor absorption lines. For example, the measured lines at 2979.97, 2985.31, 3127.13, 3138.88, and 3143.17 $cm^{-1}$ could all be assigned to ammonia lines centered—according to Hitran[44]—at 2979.943, 2985.272, 3127.100, 3138.831, and 3143.125 $cm^{-1}$, respectively. The small discrepancies between the wavenumber of measured and assigned lines are within 0.05 $cm^{-1}$. As explained previously, only one data point per line is available in a wide scan. Therefore, the lines pictured in Figure 5 are not necessarily centered on gaseous transitions. Deviations depend on the line profiles, which are not resolved in Figure 5.

Urea pyrolysis has been extensively studied in literature.[46–49] No significant reaction takes place when urea is heated from room temperature to its melting point (mp), situated at 406 K. Around

(44) Rothman, L. S.; Jacquemart, D.; Barbe, A.; Benner, D. C.; Birk, M.; Brown, L. R.; Carleer, M. R.; Chackerian, C., Jr.; Chance, K. V.; Coudert, L. H.; Dana, V.; Devi, V. M.; Flaud, J.-M.; Gamache, R. R.; Goldman, A.; Hartmann, J.-M.; Jucks, K. W.; Macki, A. G.; Mandin, J.-Y.; Massie, S. T.; Orphal, J.; Perrin, A.; Rinsland, C. P.; Smith, M. A. H.; Tolchenov, R. N.; Toth, R. A.; Vander Auwera, J.; Varanasi, P.; Wagner, G. *J. Quant. Spectrosc. Radiat. Transfer* **2005**, *96*, 139.

(45) Langer, J.; Schrader, B.; Bastian, V.; Jacob, E. *Fresenius J. Anal. Chem.* **1995**, *352*, 489.

(46) Yim, S. D.; Kim, S. J.; Baik, J. H.; Nam, I.-S.; Mok, Y. S.; Lee, J.-H.; Cho, B. K.; Oh, S. H. *Ind. Eng. Chem. Res.* **2004**, *43*, 4856.

(47) Stradella, L.; Argentero, M. *Thermochim. Acta* **1993**, *219*, 315.

(48) Schaber, P. M.; Colson, J.; Higgins, S.; Dietz, E.; Thielen, D.; Anspach, B.; Brauer, J. *Am. Lab.* **1999**, *31*, 13.

(49) Schaber, P. M.; Colson, J.; Higgins, S.; Thielen, D.; Anspach, B.; Brauer, J. *Thermochim. Acta* **2004**, *424*, 131.

425 K, it is generally accepted that urea thermally decomposes into ammonia and isocyanic acid as follows:

$$(NH_2)_2CO\,(l \text{ or } g) \rightarrow NH_3\,(g) + HNCO\,(g). \qquad (2)$$

This could explain the significant amount of ammonia measured when urea was heated up to 423 K in 100 mbar $N_2$. By comparing the intensity of several lines, it was found that the concentration of ammonia in the cell was ≥1.6%; i.e., the total amount of ammonia in the 2.0 L volume was $\geq 9.1 \times 10^{-5}$ mol. Therefore, of the 15 mg of urea ($25.6 \times 10^{-5}$ mol), at least 35% decomposed. The decomposition product isocyanic acid (HNCO) is not listed in the latest Hitran edition, but has been the subject of other rotational−vibrational studies.[50,51] The latter do not report significant isocyanic acid absorption in the spectral region covered by Figure 5. However, the elevated HNCO concentration in the cell and the long absorption path length could explain the presence of unassigned weak HNCO absorption lines reported here for the first time. (One should be careful not to confuse isocyanic acid (HNCO) with its less stable isomer cyanic acid (HOCN). A good insight on stable CHNO species can be found in literature.[51])

Other major urine organic constituents—including creatinine, uric acid, glucose, and human albumin—were investigated spectroscopically at 423 K. Uric acid does not have any C−H bond and does not reveal any absorption features in the spectral region covered by Figure 5. The texture of creatinine (mp 528 K) and human albumin after heating up to 423 K did not show any signs of decomposition. Glucose has a melting point at ~423 K. Creatinine, human albumin, and glucose had too low vapor pressures at 423 K to produce any significant absorption when 1 mg of each constituent was introduced in the HTMC vessel.

In summary, vapor-phase IR analysis of human urine in the C−H stretching region is primarily limited by the two main urine constituents, i.e., water vapor and urea. Water has strong absorption lines throughout the spectral range accessible by the DFG source, while urea thermally decomposes into ammonia and isocyanic acid. An extraction technique is therefore required for forensic analysis of urine samples.

Blank human urine matrixes came from reconstituted lyophilized or fresh specimens. Positive samples were obtained by adding the desired amount of analyte in a blank. Negative (blank) and positive urine specimens underwent the same preparation procedure described above in the Experimental Section. The vessel containing the prepared probe was sealed to the HTMC. The cell was evacuated at room temperature below $10^{-3}$ mbar for a few minutes, thereby evaporating eventual chloroform or water traces that remained in the prepared probe. The cell was filled again with 70 mbar $N_2$ and heated up to 423 K, always keeping the mirrors at a slightly higher temperature to avoid condensation on their optical surface. Vapor-phase spectra were recorded between 2900 and 3025 $cm^{-1}$ with steps of 0.4 $cm^{-1}$. The total optical path length was 31.7 m. The wide tuning range encompassed the $\nu_5$ vibrational band of ephedrine, which is clearly distinguishable from the $\nu_5$ band of pseudoephedrine (Figure 3).

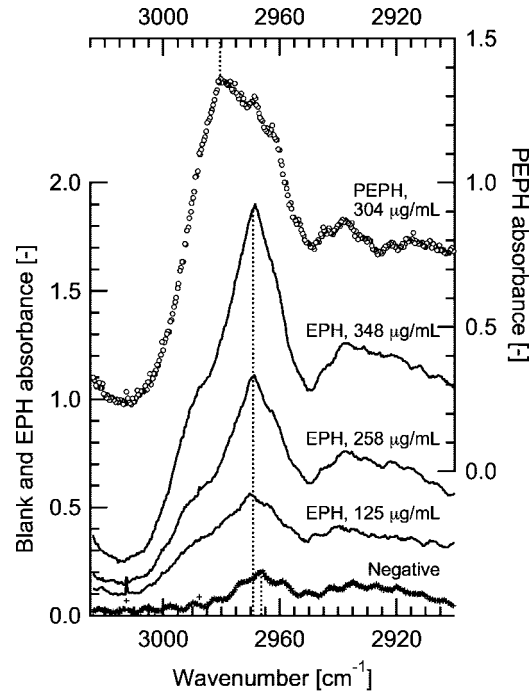


**Figure 6.** Vapor-phase infrared spectra of prepared ephedrine-positive (EPH), pseudoephedrine-positive (PEPH), and blank (negative) human urine samples. Single scans were taken in 100 mbar $N_2$ at 423 K. The spectrum of the blank exhibits fringe artifacts. The path length of the HTMC was 31.7 m. The DFG laser was tuned with steps of 0.4 $cm^{-1}$.

Ephedrine-positive probes were prepared at concentrations that were 1 order of magnitude above the legal limit. Within this range, the spectra of prepared ephedrine-positive urine samples clearly have stronger absorption features than those of a blank, as seen in Figure 6. The spectra also reveal a characteristic peak at 2969.4 ± 1 $cm^{-1}$, mainly due to the $\nu_5$ band of ephedrine. A pseudoephedrine-positive urine sample was prepared as well. It reveals strong absorption features. The main peak, situated at 2980.0 ± 0.5 $cm^{-1}$, is in good agreement with measurements taken on pure pseudoephedrine (Figure 3). Therefore, the two diastereoisomers are distinguishable even in urine.

A residual absorption is present in the blank. Its intensity varies among the different urine specimens collected, but its main peak, situated at 2966.3 ± 0.5 $cm^{-1}$, is reproducible. By means of homemade synthetic urine preparations, the origin of this absorption was investigated. It appears that an aqueous solution of urea (25 g/L as in normal urine) has the same effect as a blank in terms of absorption, whereas a prepared alkaline water solution does not produce any measurable absorption. Based on the results presented in Figure 5, it is unlikely that the measured spectrum of a blank originates from urea itself. The product of a reaction involving urea and, possibly, NaOH or chloroform rather seems to be the cause of the unknown substance extracted from a blank.

Assuming that the additional absorbance in the case of a positive sample is solely due to the doping agent, an average ephedrine recovery of 44 ± 3% can be derived.

Given an instrumental noise level of 0.3% (transmission scale) and an optical path length of 31.7 m, the absolute detection limit of pure ephedrine is 12 $\mu$g (Figure 4). With an average ephedrine recovery of 44 ± 3%, the detection limit in urine would be, in principle, 2.7 and 1.4 $\mu$g/mL if 10 and 20 mL of urine were

(50) Coffey, M. J.; Berghout, H. L.; Woods, E.; Crim, F. F. *J. Chem. Phys.* **1999**, *110*, 10850.
(51) Bondybey, V. E.; English, J. H.; Mathews, C. W.; Contolini, R. J. *J. Mol. Spectrosc.* **1982**, *92*, 431.

prepared, respectively (SNR = 3). In practice, the absorption level of a blank, however, limits the achievable detection limit to 50 and 25 $\mu$g/mL, respectively.

**Perspective Improvements.** Below, the laser spectrometer is fairly evaluated on the basis of well-known comparative criteria:

**(1) Sensitivity.** The method developed in this work could serve as a complementary tool to confirm certain positive findings, using the "B" probe of an athlete. The majority of doping agents, however, must be detectable in urine at nanogram per milliliter concentrations, requiring 3 orders of magnitude lower detection limits. The laser spectrometer has still room for much improvement: other sample preparation methods can be investigated; the length/volume ratio of the cell can be optimized; the noise level, of the order of 0.3%, is not inherently limited by the method, but by temperature deviations of the PPLN only. With the ongoing developments of broadly tunable mid-IR laser sources previously mentioned, there is no doubt that the relatively high noise level reported in this work could be significantly decreased. Given the current noise level and a maximum path length of 34.9 m inside the cell, the minimum detectable absorption coefficient (SNR = 3) is $2.6 \times 10^{-6}$ cm$^{-1}$.

**(2) Selectivity.** The main advantage of IR spectroscopy resides in its fingerprinting ability. Isomer discrimination is more accurate than in mass spectrometry. In this work, stereoisomers could be distinguished between each other even when dissolved in urine. Drug mixtures have, however, not been investigated.

**(3) Speed.** The scanning time is limited by the temperature tuning and by the waveform acquisition rate of the digital oscilloscope, which typically does not exceed 30 acquisitions/s. A boxcar or a data acquisition card could considerably accelerate the acquisition time as the frequency repetition rate of the idler laser pulses is in the kilohertz range. Furthermore, with a mid-IR source that does not rely on temperature tuning of an optical element, the time required for a wide scan could be considerably reduced. The total time to analyze a urine probe would ultimately be limited by the sample preparation procedures which, for the time being, seem inevitable.

**(4) Portability.** The reputation of laser systems as portable devices is justified. The laser spectrometer could indeed fit in a suitcase. Further miniaturization would require a direct mid-IR laser source such as an external cavity QCL.

## CONCLUSIONS

The high-temperature multipass cell combined with the widely continuously tunable DFG source offers a unique analytical tool for probing liquid and solid organic samples in the vapor phase. For example, the vapor-phase IR spectra of the diastereoisomeric pair ephedrine and pseudoephedrine can clearly be distinguished with respect to a vibrational band centered at 2970.5 and 2980.1 cm$^{-1}$, respectively. Surprisingly, the absorption features of these two stimulants are as strong as the main C−H stretching vibrational peak of acetone.[17] The effective cross section of the main pseudoephedrine peak, centered at 2980.1 cm$^{-1}$, is even as high as $2.5 \times 10^{-19}$ cm$^2$ at 423 K.

Direct examination of urine in the laser spectrometer is hindered by the strong water content of urine and the thermal degradation of urea into ammonia and isocyanic acid. However, prepared by means of liquid−liquid extraction, negative, ephedrine-positive, and pseudoephedrine-positive human urine samples can unambiguously be differentiated. The vapor-phase IR spectra of positive urine samples are consistent with previous results obtained on pure samples. With an average ephedrine recovery of 44% after solvent extraction, the detection limit of ephedrine in human urine is close to the prohibited level (10 $\mu$g/mL), i.e., 50 and 25 $\mu$g/mL, when 10 and 20 mL of urine are prepared, respectively. Infrared laser spectroscopy could therefore serve as a complementary tool to confirm certain positive findings, using the "B" probe of an athlete.

The detection limit is limited by the absorption level of a negative (blank) sample. In principle, the detection limit can be improved to ~1 $\mu$g/mL with an appropriate sample preparation procedure. The laser spectrometer has also room for much improvement with respect to the scanning time and the instrumental noise. A laser-based analytical method has thus been developed to differentiate isomers in urine at relevant concentrations without preliminary chromatographic separation. This work opens the pathway to new applications where laser-based systems could play an important role in the future.

## ACKNOWLEDGMENT

This work was entirely funded by the GEBERT RUEF STIFTUNG.

Received for review January 25, 2008. Accepted April 23, 2008.

AC8001897